Article

Analysis and Roll Prevention Control for Distributed Drive Electric Vehicles

Xiaoyu Chang, Huanhuan Zhang *, Shuai Yan, Shengli Hu and Youming Meng

School of Mechanical and Automotive Engineering, Shanghai University of Engineering Science, Shanghai 201620, China
* Correspondence: zhanghh@sues.edu.cn

Abstract: This work presents an approach to improve the roll stability of distributed drive electric vehicles (DDEV). The effect of the reaction torque from the in-wheel motor exerts additional roll moment, which is different from traditional vehicles. The additional roll moment can be achieved by active control of the wheel torque adjustment, which achieves a control effect similar to the active suspension. The anti-roll control strategy of decoupling control of roll motion and yaw motion are proposed. The direct yaw moment is calculated by the linear quadratic regulator (LQR) algorithm while the additional rolling moment is calculated by the sliding mode variable structure. For maneuvering rollover caused by excessive lateral acceleration, an anti-rollover control strategy is designed based on differential braking. A fuzzy control theory is used to decide the yaw moment to be compensated. The distribution method of the braking torque applied to the outer wheel alone, and the lateral load transfer rate is the main evaluation index for simulation verification of typical working conditions. The simulation results show that the proposed control strategy for DDEV is effective.

Keywords: distributed drive electric vehicles; additional roll moment; decoupling control; load transfer rate

1. Introduction

In recent years, the problem of environmental pollution and energy shortage caused by the massive use of fossil energy has become increasingly serious. The traditional automobile belongs to the industry of high energy consumption and high pollution. Therefore, more and more researchers and enterprises engaged in automobile related work focus on electric vehicles. Distributed drive electric vehicles (DDEV) are one kind of electric vehicles, and the research and development of its key technologies has always been the focus of many automotive and industrial experts. Compared with traditional fuel vehicles, there is no transmission system to transmit power in the distributed drive electric vehicle (DDEV). It not only enables the vehicle to have more controllable degrees of freedom, but also greatly improves its efficiency and response speed, which helps to solve the sustainability problems of energy and vehicles. In [1] a study using bibliometric analysis, analyses sustainable mobility in relation to economic returns, environmental benefits and societal advantages.

The rollover accidents caused by the loss of the stability of vehicles seriously threaten people's lives, property and safety. It has become a safety issue and attracted worldwide attention. The statistics of the US Highway Traffic Safety Administration show that the degree of harm caused by vehicles rollover accidents are second only to vehicles collision accidents in all traffic accidents [2]. Many scholars all over the word have conducted research on the vehicle roll motion control, including controlling the body posture and changing the trajectory of the vehicles. Body posture control can be subdivided into lateral stabilizer control [3–5] and active suspension control [6,7] while the trajectory change strategy consists of active steering control [8–11] and differential brake control [12,13].

The unique structure of DDEV affects the roll and rollover performance which includes the following aspects: (1) in-wheel motors increase the unsprung mass, which will

deteriorate the vibration isolation performance of the suspension and cause the lifting effect of the wheels; (2) because of rigid connection between the suspension and the motor stator, the ground driving force and the reaction torque of the motor to be transmitted to the body will form a large roll torque; (3) The cancellation of the differential will cause the coaxial drive wheels to lose the torque self-balancing mechanism. The torque difference between the two sides of the wheels form a large yaw moment. It will cause excessive steering of the car or sharp turn. Therefore, to study the roll stability of the DDEV is the basis and premise for proposing the anti-rollover control [14].

Currently, the safety control of DDEV is mainly focused on the yaw stability. However, many studies on the roll stability control are mainly to control the suspension. Among them, the literature [15] aimed at the roll phenomenon of in-wheel driving vehicles. Based on the control of the suspension technology through the vertical load distribution transfer, the vehicle's front and rear axle lateral stiffness are changed. In [16] an active suspension control algorithm was designed based on the optimal control theory LQG and the robust control theory respectively. According to the driving status, the extra force is applied to the suspension to reduce the dynamic displacement. It made the vertical motion in an optimal state. However, the active suspension is both expensive and complex. Consequently, other control schemes have been developed to maintain the roll stability. A strategy of applying driving/braking torque to different drive motors is proposed in [17,18]. An additional roll moment is generated to the vehicle's body that effectively improves the posture of the vehicle body. A roll stability controller is designed in literature [19], which takes the suppression of the body's roll angle as the control target and its roll torque was generated by the wheel drive torque difference, so it is no longer necessary to design a separate suspension actuator. A joint control system for roll stability and yaw stability is designed in literature [20]. The controller considered the coupling effect of yaw rate and lateral acceleration. The adjustment factor RI is proposed to allocate the proportion of the roll control, which effectively improved the roll stability of the vehicle. Integrated control of the roll, yaw and pitch of DDEV was implemented in literature [21]. It based on the algorithm of optimal allocation of different wheel torques. The strategy did not require the analysis of complex equations to achieve spatial stability of the vehicle. The additional roll moment force of DDEV is analyzed in literature [22]. It is generated by the driving/braking torque. The in-wheel motor drive itself has the ability to self-adjust the body posture, it is found.

It should be noted that different driving torque could realize the control of the rolling moment. Its effect is similar to the active suspension. But the roll and yaw of the vehicle will affect each other to exacerbate the instability of the vehicle. In this paper, the anti-roll control strategy for decoupling control of roll and yaw is proposed. For the roll torque generated by the centrifugal force due to excessive lateral acceleration and centrifugal force, an anti-rollover control strategy for differential braking is proposed.

Section 2 analyzes the generating mechanism of the DDEV roll moment. Section 3.1 discusses the rolling stability control based on active distribution of wheel driving torques. The change of wheel driving torque will affect both the vehicle's roll stability and yaw stability, so the anti-roll control strategy for decoupling control of roll motion and yaw motion is proposed, which is the main contribution of this work. Aiming at the maneuvering rollover caused by excessive roll acceleration, an anti-rollover control strategy based on differential braking is proposed, which is in Section 3.2. Section 4 shows the behavior of the control system in a simulation environment.

2. Generating Mechanism of the Rolling Moment of DDEV
2.1. Rolling Moment of DDEV

The vehicles' rolling moment is mainly composed of three parts. The first term represents the rolling moment caused by the centrifugal force of the sprung mass. The second term is caused by the deviation of the spring center of gravity The third term is produced by the force of the suspension on the body [23].

DDEV also produces the above three kinds of rolling moments when turning. The interaction between the vehicle body and the suspension has a great impact for the rolling moment. After introducing the in-wheel motor, the ground driving force and the reaction torque of the motor are transmitted to the body through the wheels and suspension, thereby generating additional "vertical force", as shown in Figure 1. In the case that the lateral acceleration is not large, the value of the roll moment generated by this "vertical force" is sufficiently large compared to the rolling moment due to lateral acceleration. The additional rolling moment will have a greater impact on the roll attitude of the vehicle body. The roll motion equation of the DDEV is expressed as

$$I_x \ddot{\phi} = m_s h_s a_y + m_s h_s g \sin \phi - (K_\phi \phi + C_\phi \dot{\phi}) - \Delta M_X \tag{1}$$

where I_x is the rotational inertia of the vehicle around the x axis; φ is vehicle roll angle; m_s is vehicle sprung mass; h_s is the distance from the center of the sprung mass to the roll center of the car; a_y is lateral acceleration at the center of mass; g is gravitational acceleration; K_φ is the equivalent roll stiffness of the vehicle; C_φ is equivalent roll damping of automobile and ΔM_X is additional roll moment.
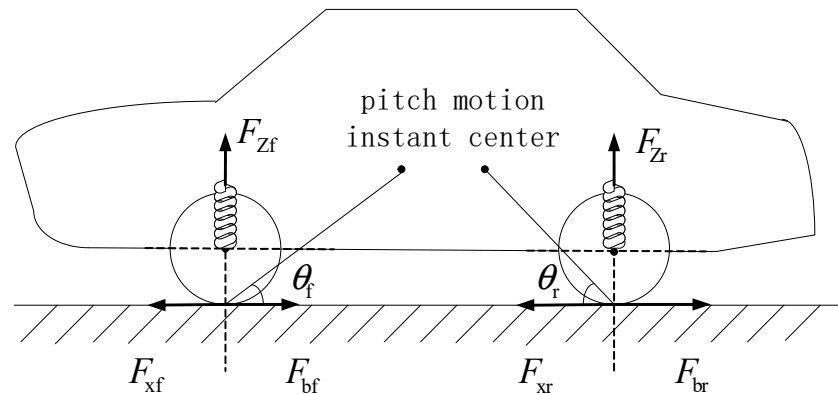
Figure 1. The diagram of additional vertical force.

2.2. Analysis of the Rolling Effect for the Additional Vertical Force of DDEV

Taking the vehicle turning left as an example, the transmission process of the additional vertical force in the longitudinal plane and the lateral plane of the vehicle is analyzed separately. The following assumptions are made:

(1) The left and right sides of the vehicle are symmetrical, and the front wheel angle δ is not large, that is, $\cos\delta \approx 1$, $\sin\delta \approx 1$;

(2) McPherson suspension is used for front and rear suspension;

(3) The loss is ignored during force or torque transmission.

In the longitudinal plane of the vehicle, the left suspension is used as a force body, the force is shown in Figure 2.
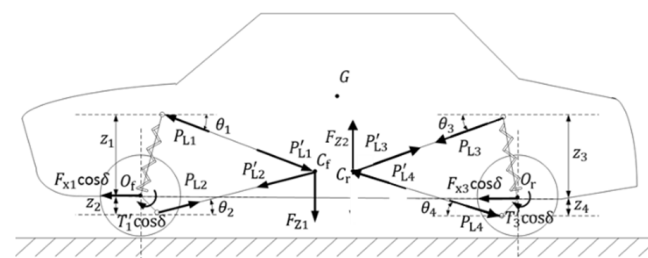
Figure 2. The force analysis of vehicle longitudinal plane.

At the center of the front left wheel O_f, the force balance equation and the moment balance equation can be obtained as

$$\begin{cases} F_{x1}\cos\delta + P_{L1}\cos\theta_1 - P_{L2}\cos\theta_2 = 0 \\ T_1\cos\delta - P_{L1}z_1/\cos\theta_1 - P_{L2}z_2/\cos\theta_2 = 0 \end{cases} \tag{2}$$

where, F_{x1} and T_1 represent the ground driving force and motor torque transmitted from the front wheel to the vehicle body via the suspension; P_{Li} (i = 1, 2) is the force exerted by the left body on the front suspensions; z_i (i = 1, 2) and θ_i (i = 1, 2) are the corresponding distance and angle in the Figure 2.

According to Equation (1), P_{L1}, P_{Li}' and P_{L2}, P_{Li}' can be expressed as

$$\begin{cases} P_{L1}' = P_{L1} = \frac{T_1\cos\delta\cos\theta_1\cos^2\theta_2 - F_{x1}\cos\delta\cos\theta_1 z_2}{z_1\cos^2\theta_2 + z_2\cos^2\theta_1} \\ P_{L2}' = P_{L2} = \frac{T_1\cos\delta\cos^2\theta_1\cos\theta_2 + F_{x1}\cos\delta\cos\theta_2 z_1}{z_1\cos^2\theta_2 + z_2\cos^2\theta_1} \end{cases} \tag{3}$$

where, P_{Li} (i = 1, 2) and P_{Li}' (i = 1, 2) are acting force and reaction force; P_{Li}' (i = 1, 2) is the force exerted by the front suspensions on the left body.

Then the vertical force of the left front wheel transmitted to the body through the suspension in the longitudinal plane can be described as

$$F_{Z1} = P_{L1}'\sin\theta_1 + P_{L2}'\sin\theta_2 \tag{4}$$

The roll moment generated by the left front wheel via the suspension in the longitudinal plane can be described as

$$M_{X1} = \frac{1}{2}BF_{Z1} = F_{x1}\frac{B\cos\delta[\sin\theta_1\cos\theta_1(\text{rcos}^2\theta_2 - z_2) + \sin\theta_2\cos\theta_2(\text{rcos}^2\theta_1 + z_1)]}{2(z_2\cos^2\theta_1 + z_1\cos^2\theta_2)} \tag{5}$$

where r is the wheel rolling radius; B is track width.

The Equation (5) can be abbreviated as

$$M_{X1} = K_1 F_{x1} \tag{6}$$

where $K_1 = \frac{B\cos\delta[\sin\theta_1\cos\theta_1(\text{rcos}^2\theta_2 - z_2) + \sin\theta_2\cos\theta_2(\text{rcos}^2\theta_1 + z_1)]}{2(z_2\cos^2\theta_1 + z_1\cos^2\theta_2)}$ Similarly, the roll moment generated by wheel via the suspension in the longitudinal plane can be described as

$$\begin{cases} M_{X1} = K_1 F_{x1} \\ M_{X2} = K_2 F_{x2} \\ M_{X3} = K_3 F_{x3} \\ M_{X4} = K_4 F_{x4} \end{cases} \tag{7}$$

where M_{X1} is the roll moment the left front wheel; M_{X2} is the roll moment of the left rear wheel; M_{X2} is the roll moment of the right front wheel; M_{X4} is the roll moment of the right rear wheel; K_i (i = 1, 2, 3, 4) is the corresponding coefficient.

The force of lateral plane is shown in Figure 3.

At the connection point of the inner suspension kingpin, there is

$$\begin{cases} F_{x1}\sin\delta + P_{i1}\cos\theta_{i1} - P_{i2}\cos\theta_{i2} = 0 \\ T_1\sin\delta - P_{i1}z_{i1}/\cos\theta_{i1} - P_{i2}z_{i2}/\cos\theta_{i2} = 0 \end{cases} \tag{8}$$

where P_{i1} and P_{i2} represent the force exerted by the vehicle body on the inner side of the front suspension; z_{i1} and z_{i2} are the corresponding distance; θ_{i1} and θ_{i2} are the corresponding angle.

P_{i1}, $P_{i1}{}'$ and, P_{i2}, $P_{i2}{}'$ can be expressed as

$$\begin{cases} P_{i1}{}' = P_{i1} = \dfrac{T_1 \sin \delta \cos \theta_{i1} \cos^2 \theta_{i2} - F_{x1} \sin \delta \cos \theta_{i1} z_{i2}}{z_{i1} \cos^2 \theta_{i2} + z_{i2} \cos^2 \theta_{i1}} \\ P_{i2}{}' = P_{i2} = \dfrac{T_1 \sin \delta \cos^2 \theta_{i1} \cos \theta_{i2} + F_{x1} \sin \delta \cos \theta_{i2} z_{i1}}{z_{i1} \cos^2 \theta_{i2} + z_{i2} \cos^2 \theta_{i1}} \end{cases} \tag{9}$$

where, P_{ij} (j = 1, 2) and P_{ij} (i = 1, 2) are a pair of acting force and reaction force, and P_{ij} (i = 1, 2) are the force exerted by the front-inner suspension on the vehicle body.
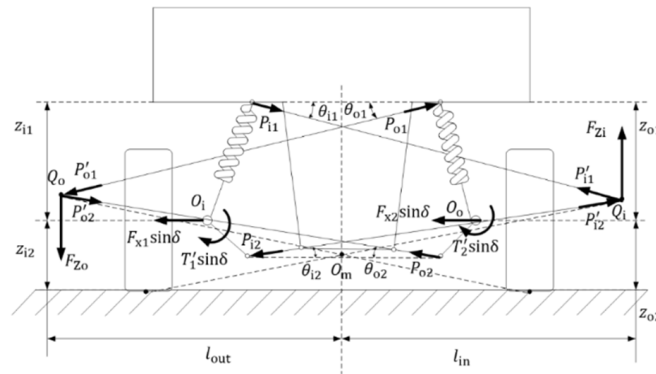
Figure 3. The force analysis of roll mechanism of lateral plane.

Then the vertical force transmitted by the front inner wheel to the body through the suspension in the transverse plane can be expressed as

$$F_{Zi} = P_{i1}{}' \sin \theta_{i1} + P_{i2}{}' \sin \theta_{i2} \tag{10}$$

And the roll moment generated by the front-inner wheel via the suspension in the transverse plane to the vehicle body is stated as

$$M_{Xi} = -(P_{i1}{}' \sin \theta_{i1} + P_{i2}{}' \sin \theta_{i2}) \cdot l_{in} \tag{11}$$

where, l_{in} is the distance from the roll center to the instantaneous center of roll motion on the inside of the front suspension.

Similarly, the roll moment generated by the front-outer wheel via the suspension is stated as

$$M_{Xo} = -(P_{o1}{}' \sin \theta_{o1} + P_{o2}{}' \sin \theta_{o2}) \cdot l_{out} \tag{12}$$

where $P_{o1}{}'$ and $P_{o2}{}'$ represent the force exerted by the front-outer suspension on the vehicle body, l_{out} is the distance from the roll center to the instantaneous center of roll motion on the outside of the front suspension, θ_{o1} and θ_{o2} are the corresponding angle.

According to the method of solving Equation (6), we can get

$$\begin{cases} M_{Xi} = K_5 F_{x1} \\ M_{Xo} = K_6 F_{x2} \end{cases} \tag{13}$$

where K_5 and K_6 are the coefficient term of the roll moment generated by the front-inner wheel and front-outer wheel.

Conclusively, the roll moment acting on the body of the DDEV can be changed by controlling the magnitude of the driving torque of the motor, so as to achieve the function of adjusting the body posture.

Based on the above analysis, it is plain that the roll posture control of the DDEV during cornering can be achieved by actively adjusting the size of the wheel driving torque.

3. Roll Stability Control Algorithm

3.1. Yaw and Roll Decoupling Control Algorithm

When the lateral acceleration is not large, the rolling effect of the vehicle body can be controlled by the wheel torque. However, the size of the wheel driving torque also directly affects the yaw moment of the vehicle, which affects the yaw stability. The distribution of the driving torque of each DDEV wheel must be comprehensive consideration of the vehicle's yaw stability and roll stability.

3.1.1. Yaw Stability Control

The linear two-degree-of-freedom vehicle can explain the vehicle's handling characteristics. The ideal side angle of mass center and ideal yaw rate of the vehicle can be expressed as

$$\beta_{\mathrm{d}} = \frac{b + mav_x^2/k_{\mathrm{r}} \cdot L}{L \cdot (1 + Kv_x^2)} \cdot \delta \tag{14}$$

$$\omega_{\mathrm{rd}} = \frac{v_x/L}{1 + K \cdot v_x^2} \cdot \delta \tag{15}$$

where, b is distance from center of mass to rear axle, a is distance from center of mass to front axle, m is the vehicle quality, v_x is the vehicle's longitudinal speed, k_r is the cornering stiffness of the rear wheel, k_f is the cornering stiffness of the front wheel, L is the vehicle wheelbase and K is the stability factor, $K = \frac{m}{L^2}\left(\frac{a}{k_{\mathrm{r}}} - \frac{b}{k_{\mathrm{f}}}\right)$.

However, the vehicle will not be always in the small-angle operation. When the tire model is in the nonlinear region, the steady-state response value of the two-degree-of-freedom vehicle model is not suitable for the ideal value. It should be replaced by the limit value. The size of the limit is constrained by the road surface adhesion coefficient μ. Considering these factors, the ideal yaw angular velocity and the ideal centroid lateral declination angle can be expressed as

$$|\omega| = \min\{|\omega_{rd}|, |\omega_{r\max}|\} \cdot sign(\delta) \tag{16}$$

$$|\beta| = \min\{|\beta_{rd}|, |\beta_{r\max}|\} \cdot sign(\delta) \tag{17}$$

where $\omega_{r\max} = \frac{\mu g}{v_x}$ and $\beta_{r\max} = \tan^{-1}(0.02\mu g)$.

The state space equation of the linear two-degree-of-freedom vehicle model take the ideal yaw rate ω_{rd} and ideal side slip angle β_d as state variables described as

$$\begin{bmatrix} \dot{\beta}_{\mathrm{d}} \\ \dot{\omega}_{\mathrm{rd}} \end{bmatrix} = \mathbf{A} \cdot \begin{bmatrix} \beta_{\mathrm{d}} \\ \omega_{\mathrm{rd}} \end{bmatrix} + \mathbf{B} \cdot (\delta) \tag{18}$$

where $\mathbf{A} = \begin{bmatrix} \frac{k_{\mathrm{f}} + k_{\mathrm{r}}}{mv_x} & \frac{ak_{\mathrm{f}} - bk_{\mathrm{r}}}{mv_x^2} - 1 \\ \frac{ak_{\mathrm{f}} - bk_{\mathrm{r}}}{I_z} & \frac{a^2k_{\mathrm{f}} + b^2k_{\mathrm{r}}}{I_z v_x} \end{bmatrix}$, $\mathbf{B} = \begin{bmatrix} -\frac{k_{\mathrm{f}}}{mv_x} & -\frac{ak_{\mathrm{f}}}{I_z} \end{bmatrix}^T$, and I_z is the moment of inertia of the vehicle around the Z axis.

The yaw instability of the vehicle mostly occurs in the non-linear region of the tire. At this time, the lateral force of the tire is gradually saturated, and the vehicle begins to appear side slip phenomenon, which deviates from the driver's desired trajectory. At this time, the vehicle can be actively compensated for an additional direct yaw moment ΔMz to make the vehicles' yaw rate ω_r and side slip angle β re-track the change of the ideal value. The relationship between the vehicle's steering characteristics and the compensated additional yaw moment is shown in Table 1.

Table 1. Relationship between vehicle steering and additional yaw moment.

Steering Condition	Yaw Velocity	Additional Yaw Moment
left understeer	$\omega_r > 0$	$\Delta M_z > 0$
left oversteer	$\omega_r > 0$	$\Delta M_z < 0$
light understeer	$\omega_r < 0$	$\Delta M_z < 0$
light oversteer	$\omega_r < 0$	$\Delta M_z > 0$

With the actual yaw velocity ω_r and the actual side slip angle β as state variables, the equation of state of automobile motion described as

$$\begin{bmatrix} \dot{\beta} \\ \dot{\omega}_r \end{bmatrix} = \mathbf{A} \cdot \begin{bmatrix} \beta \\ \omega_r \end{bmatrix} + \mathbf{B} \cdot (\delta) + \mathbf{B}_1 \cdot \Delta M_Z \tag{19}$$

where, ΔM_z is additional direct yaw moment, and $\mathbf{B}_1 = [0 \ 1/I_z]^{\mathbf{T}}$.

Subtract (19) from (18), we can get the following Equation

$$\begin{bmatrix} \Delta\dot{\beta} \\ \Delta\dot{\omega}_r \end{bmatrix} = \mathbf{A} \cdot \begin{bmatrix} \Delta\beta \\ \Delta\omega_r \end{bmatrix} + \mathbf{B}_1 \cdot \Delta M_z \tag{20}$$

where $\Delta\beta$ is the difference between the actual side slip angle and the ideal side slip angle; $\Delta\omega_r$ is the difference between the actual yaw velocity and the ideal yaw velocity.

Equation (20) describes the dynamic relationship between the direct yaw moment and the yaw velocity deviation and the side slip angle deviation. So the optimal direct yaw moment [24–26] can be determined by LQR control theory as

$$\Delta M_Z = -\mathbf{K}\mathbf{x}(t) = -k_1 \Delta\beta(t) - k_2 \Delta\omega_r(t) \tag{21}$$

where $\mathbf{K}$ is the feedback matrix, and $\mathbf{K} = [k_1 \ k_2]^{\mathbf{T}}$.

3.1.2. Roll Stability Control

Aiming at the roll phenomenon of the vehicle body, an active control strategy is applied to improve the roll attitude of the vehicle when cornering. Based on the sliding mode variable structure control theory, this paper implements the design of the roll stability controller. It can be seen from the three-degree-of-freedom vehicle model of DDEV that its roll motion equation is as follows

$$I_x \ddot{\phi} = m_s h_s (\dot{v}_y + v_x \omega_r) + m_s h_s g \sin\phi - (K_\phi \phi + C_\phi \dot{\phi}) - \Delta M_X \tag{22}$$

where v_y is the vehicle lateral speed.

When the body has a serious roll instability phenomenon, according to the Equation (22), the vehicle can be compensated with an anti-roll moment ΔM_X to recover the roll stability.

In order to reduce the roll angle and roll velocity, the sliding mode surface can be defined as

$$s = \dot{e} + \xi e \tag{23}$$

where, ξ is the weight coefficient between the roll angle and roll angular velocity; e is the error of roll angle.

Derivation of Equation (23) can be obtained

$$\dot{s} = \ddot{\phi} + \xi\dot{\phi} \tag{24}$$

The additional rolling moment is expressed as

$$\Delta M_X = m_s h_s (\dot{v}_y + v_x \omega_r) + (\xi I_x - C_\phi)\dot{\phi} + (m_s h_s g \sin\phi - K_\phi)\phi + \eta sat(s) \tag{25}$$

where *sat(s)* is the saturation function; η is the switching gain.

3.1.3. Torque Distribution Strategy for Decoupling Control

Assuming that the vehicle is in an unstable state, the yaw moment to be compensated is ΔM_z, and the roll moment to be compensated is ΔM_x, and the yaw moment and roll moment that can be compensated by adjusting the driving torque of each wheel are shown in Table 2 respectively.

Table 2. Compensating roll and yaw moment for 4 wheels.

Wheel	Compensated Roll Moment	Compensated Yaw Moment
front left wheel torque	ΔM_{X1}	ΔM_{Z1}
rear left wheel torque	ΔM_{X3}	ΔM_{Z3}
front right wheel torque	ΔM_{X2}	ΔM_{Z2}
rear right wheel torque	ΔM_{X4}	ΔM_{Z4}

The distribution of the roll moment is as follows

$$\begin{cases} \Delta M_{X1} + \Delta M_{X3} = \Delta M_X/2 \\ \Delta M_{X2} + \Delta M_{X4} = \Delta M_X/2 \end{cases} \tag{26}$$

The distribution of the yaw moment is as follows

$$\begin{cases} \Delta M_{Z1} + \Delta M_{Z3} = \Delta M_Z/2 \\ \Delta M_{Z2} + \Delta M_{Z4} = \Delta M_Z/2 \end{cases} \tag{27}$$

Suppose that the increment of driving force applied to each wheel is as follows

$$\begin{cases} \Delta M_{X1} = K_1 \Delta F_{x1} + K_5 \Delta F_{x1} \\ \Delta M_{X2} = K_2 \Delta F_{x2} + K_6 \Delta F_{x6} \\ \Delta M_{X3} = K_3 \Delta F_{x3} \\ \Delta M_{X4} = K_4 \Delta F_{x4} \end{cases} \tag{28}$$

$$\begin{cases} \Delta M_{Z1} = -\frac{1}{2} B \Delta F_{x1} \cos \delta + \Delta F_{x1} \sin \delta \cdot a \\ \Delta M_{Z2} = \frac{1}{2} B \Delta F_{x2} \cos \delta + \Delta F_{x2} \sin \delta \cdot a \\ \Delta M_{Z3} = -\frac{1}{2} B \Delta F_{x3} \\ \Delta M_{Z4} = \frac{1}{2} B \Delta F_{x4} \end{cases} \tag{29}$$

According to Equations (26)–(29), the driving force distribution strategy of the inner and outer wheels can be solved as in the following.

Inside wheels:

$$\begin{cases} K_1 \Delta F_{x1} + K_5 \Delta F_{x1} + K_3 \Delta F_{x3} = \Delta M_X/2 \\ -\frac{1}{2} B \Delta F_{x1} \cos \delta + \Delta F_{x1} \sin \delta \cdot a - \frac{1}{2} B \Delta F_{x3} = \Delta M_Z/2 \end{cases} \tag{30}$$

Outer wheels:

$$\begin{cases} K_2 \Delta F_{x2} + K_6 \Delta F_{x2} + K_4 \Delta F_{x4} = \Delta M_X/2 \\ \frac{1}{2} B \Delta F_{x2} \cos \delta + \Delta F_{x2} \sin \delta \cdot a + \frac{1}{2} B \Delta F_{x4} = \Delta M_Z/2 \end{cases} \tag{31}$$

Rewrite equation (30) and equation (31) into the following matrix form:

$$\mathbf{Ax} = \mathbf{B} \tag{32}$$

where, $\quad\mathbf{K} \quad = \quad [\Delta F_{x1} \quad \Delta F_{x2} \quad \Delta F_{x3} \quad \Delta F_{x4}]^{\mathbf{T}}$

$$\mathbf{A} = \begin{bmatrix} K_1 + K_5 & 0 & K_3 & 0 \\ -\frac{1}{2}B\cos\delta + \sin\delta \cdot a & 0 & -\frac{1}{2}B & 0 \\ 0 & K_2 + K_6 & 0 & K_4 \\ 0 & \frac{1}{2}B\cos\delta + \sin\delta \cdot a & 0 & \frac{1}{2}B \end{bmatrix},$$

$\mathbf{B} = \begin{bmatrix} \Delta M_X/2 & \Delta M_Z/2 & \Delta M_X/2 & \Delta M_Z/2 \end{bmatrix}^{\mathbf{T}}$.

Considering the limitation of motor power and pavement condition, ΔF_{xi} should meet the limits as following:

$$\begin{cases} |\Delta F_{xi} \cdot r| \leq T_{\max} \\ |\Delta F_{xi} \cdot r| \leq \mu mg \end{cases} \tag{33}$$

where ΔF_{xi} is the increment of each driving force. r is the radius of the wheel; $T_{\max}$ is the maximum driving moment of the motor; μ is the road adhesion coefficient.

And the increment of each wheel drive torque can be expressed as following:

$$\begin{cases} \Delta T_1 = \Delta F_{x1} \cdot r \\ \Delta T_2 = \Delta F_{x2} \cdot r \\ \Delta T_3 = \Delta F_{x3} \cdot r \\ \Delta T_4 = \Delta F_{x4} \cdot r \end{cases} \tag{34}$$

Finally, the decoupling control of the roll stability and yaw stability of the DDEV can be achieved by distributing the increment of the driving torque of each wheel.

3.2. Anti-Rollover Control Algorithm Based on Differential Brake

On a good level road with high adhesion coefficient, the lateral acceleration of the vehicle can reach more than 0.8 g when turning. At the same time, the centrifugal force of the vehicle is large enough, which is likely to cause rollover. Although DDEV can control the vehicle's roll attitude by controlling the driving force, it is difficult to avoid the vehicle rollover phenomenon only by controlling the driving force in an emergency situation of high-speed sharp turns. Applying brake control and reducing the speed are often the safest control strategy.

As shown in Figure 4, the brake control is applied to the target wheels by differential braking. The fuzzy controller outputs the compensated yaw moment, and the torque distribution controller outputs the braking pressure applied on the front outer wheel.
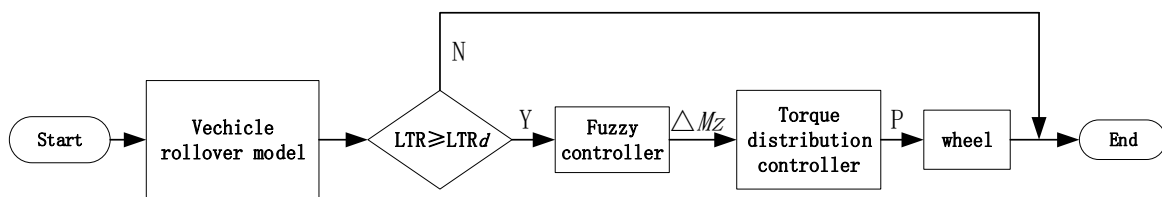
Figure 4. Anti-rollover control flow.

The vehicle's longitudinal speed will obviously change after performing differential brake control. At the time, the vehicle model should be extended from three-degree-of-freedom vehicle model to four-degree-of-freedom vehicle model, and the equation of motion is

$$\begin{cases} m\dot{v}_x = F_b \\ ma_y = F_{yf} + F_{yr} \\ I_z\dot{\omega}_r = aF_{yf} - bF_{yr} + \Delta M_Z \\ I_x\ddot{\phi} = m_s h_s a_y + m_s h_s g \sin\phi - K_\phi\phi - C_\phi\dot{\phi} \end{cases} \tag{35}$$

where F_b represents the braking force exerted on the front outer wheel, a_y is the vehicle lateral acceleration, F_{yf} and F_{yr} are the side force of vehicle front and rear wheels, ΔM_Z represents the compensated additional yaw moment.

We can get from Equation (35) that the essence of differential braking control is applying a braking force to the front outer wheel to make the vehicle generate an additional yaw moment. The longitudinal speed and yaw rate will be improved. Obviously, the correctness of the additional yaw moment is directly related to the quality of the control effect. ΔM_Z will be calculated by fuzzy control algorithm.

3.2.1. Evaluation Index of Vehicle Rollover

LTR is used as the evaluation index of vehicle rollover [15]. The definition of LTR is

$$\text{LTR} = \frac{(F_{z1} + F_{z3}) - (F_{z2} + F_{z4})}{F_{z1} + F_{z2} + F_{z3} + F_{z4}} \tag{36}$$

where F_{z1}, F_{z2}, F_{z3} and F_{z4} are the vertical load of each driving wheel.

When LTR = 0, it means that the vertical load on the left and right sides of the vehicle is equal, and there is no roll phenomenon;

When LTR = 1, it means that the vertical load of the right wheel is just 0, and the vehicle has a tendency to turn to the left;

When LTR = -1, it means that the vertical load of the left wheel is just 0, and the vehicle has a tendency to turn to the right.

The value of the lateral load transfer rate LTR should be as close to 0 as possible. In order to prevent the vehicle from entering a rollover state, LTR should be satisfied that $|\text{LTR}| \leq 1$. In general, $|\text{LTR}| = 0.8$ is taken as the critical state of automobile rollover to ensure the safety of the vehicle and prevent the negative impact of excessive lateral load transfer.

3.2.2. Fuzzy Control Algorithm

Fuzzy control is a control method based on fuzzy mathematics. Its great advantage is that it does not require accurate mathematical models. A series of variables describing the driving state of the vehicle such as the yaw rate, the side angle, the roll angle and the lateral acceleration are difficult to express with a precise mathematical equation. At this time, the concept of fuzzy mathematics can be used to deal with similar control problems. The fuzzy controller outputs the compensated yaw moment ΔM_Z who is entered into torque distribution controller. The torque distribution controller outputs the braking pressure applied on the front outer wheel.

And the fuzzy rules in this paper are listed in Table 3.

Table 3. Fuzzy control rule table.

ΔM_Z		e						
		NB	**NM**	**NS**	**ZO**	**PS**	**PM**	**PB**
	PB	ZO	ZO	NW	NS	NM	NB	NB
	PS	PM	PS	ZO	NW	NS	NB	NB
ec	ZO	PB	PM	PW	ZO	NW	NM	NB
	NS	PB	PB	PS	PW	ZO	NS	NM
	NB	PB	PB	PM	PS	PW	ZO	ZO

3.2.3. Distribution Strategy of Yaw Moment

Taking the vehicle turning left as an example to illustrate the distribution strategy of compensated yaw moment ΔM_Z. When the vehicle is in danger of rollover, a braking torque will be applied to the right front wheel of the vehicle separately. The relationship between compensated yaw moment and braking force is

$$F_b\left(\frac{B}{2}\cos\delta + a\sin\delta\right) = \Delta M_Z \tag{37}$$

The kinematic equation of the right front wheel during braking is as follows

$$I_w\dot{\omega} = T_b - F_b r \tag{38}$$

where I_w is the rotating inertia of front outer wheel; ω is the angular velocity of the wheel; T_b is the vehicle braking torque.

The mathematical expressions of braking torque and wheel cylinder pressure of the braking system are as following:

$$T_b = S \cdot P \tag{39}$$

where P is the braking pressure; S is the braking efficiency coefficient.

The relationship between the yaw moment and brake pressure can be obtained from Equations (37)–(39) as following:

$$P = \frac{1}{S}\left(\frac{2 \cdot r \cdot \Delta M_Z}{B\cos\delta + 2a\sin\delta} + I_w\dot{\omega}\right) \tag{40}$$

As long as the braking pressure of the size P is applied to the front outer wheels, the vehicle can generate an additional yaw moment according to the Equation (40), so that the DDEV can achieve the effect of anti-rollover control.

4. Simulation and Verification

4.1. Vehicle Model

The 18 DOF vehicle model established in literature [27] is used in this paper. 6 freedoms of vehicle body, 4 vertical freedoms for suspension, 4 rotary motion freedoms and 4 vertical freedoms of wheels are included. The main simulation parameters of the vehicle model are shown in Table 4.

Table 4. Main parameters of vehicle model.

Parameters	Value
Vehicle mass	1380
sprung mass	900
un-sprung mass	480
Distance from center of mass to front axle	1.05
Distance from center of mass to rear axle	1.57
front wheel tread	1.4
rear wheel tread	1.4
height of centroid	0.6
Tire diameter load radius	0.33
tire type	255/75 R16

The Magic-Formula tire model is used as the tire model. The brushless DC motor is selected as the driving motor of the vehicle. Since the research is focused on the roll stability of the vehicle, the motor torque control can be simplified into the transfer function model of the actual electromagnetic torque T_m to the target electromagnetic torque $T_m{}^*$. The transfer function is

$$G(s) = \frac{T_m(s)}{T_m^*(s)} = \frac{1}{2\zeta^2 s^2 + 2\zeta s + 1} \tag{41}$$

where ξ is determined by motor characteristics, it can be obtained by fitting test results.

4.2. Simulation Verification of Yaw and Roll Decoupling Control Algorithm

4.2.1. Angular Step Input Condition

At speed of 60 km/h input the steering wheel angle which set to 50°, and the road surface adhesion coefficient is set to 0.25. The simulation results are shown in Figure 5.

(a)

(b)

(c)

(d)

(e)

(f)
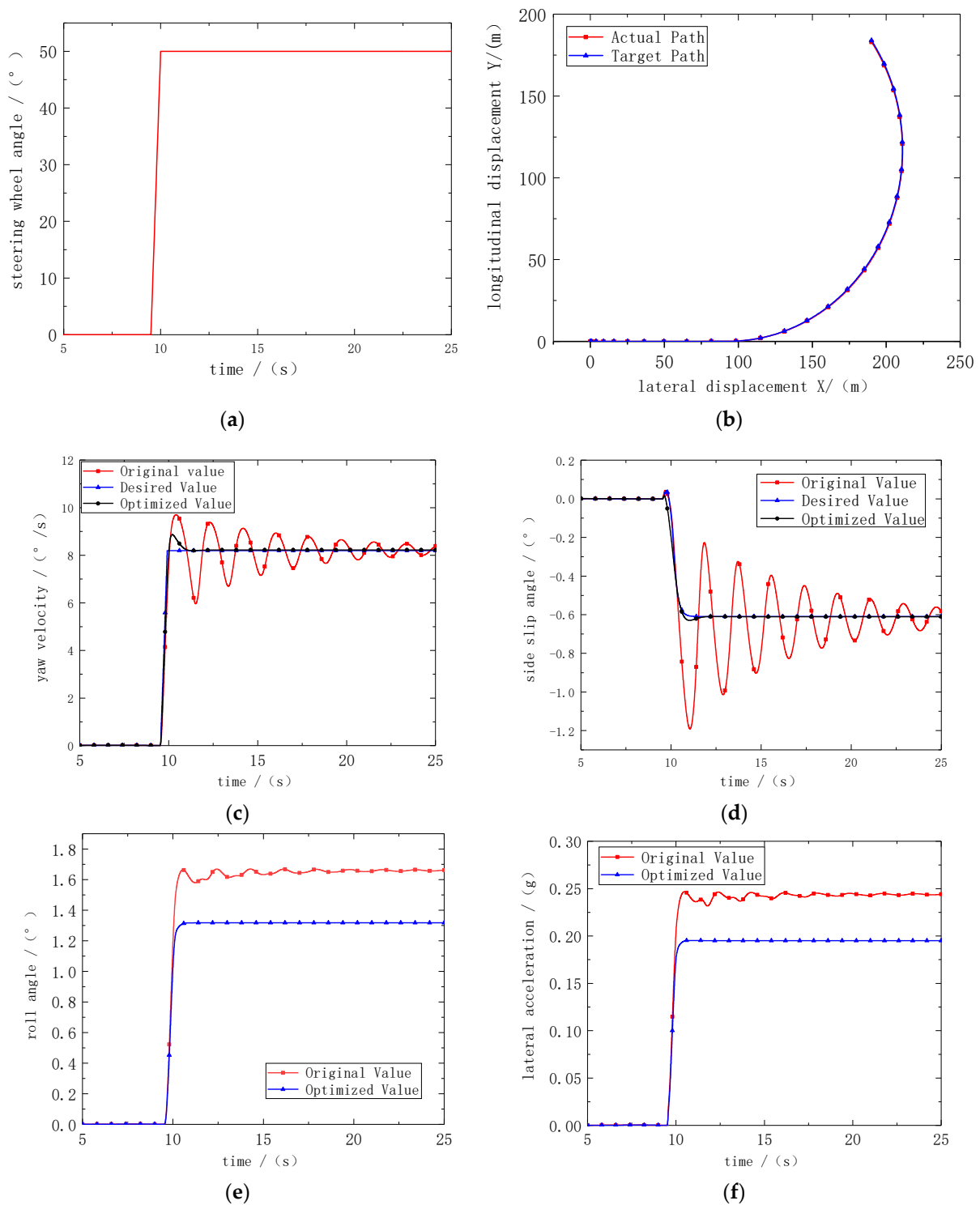
Figure 5. Simulation results of angular step input condition. (**a**) Steering wheel angle. (**b**) Vehicle track. (**c**) Yaw velocity. (**d**) Side slip angle. (**e**) Lateral acceleration. (**f**) Roll angle.

Figure 5b shows the change of the trajectory of the vehicle before and after the control. There is no obvious difference between the two curves, indicating that the vehicle is not completely unstable; Figure 5c,d show the yaw rate and the side slip angle of the vehicle respectively. After the control strategy is applied, the vehicle's yaw rate and side slip angle can ideally track the change of the ideal value. When the control strategy is not applied, both the yaw rate and side slip angle of show large fluctuations. It indicates that the vehicle has not completely destabilized. The controller can control the vehicle's lateral

well under this condition showed by Figure 5e,f. It can be seen that the roll angle of the vehicle is reduced by about 80% after the control is applied, and the lateral acceleration is also suppressed to a certain extent. In summary, the roll and yaw decoupling controller designed in this paper can gradually stabilize the vehicle that is not completely unstable under the angular step condition.

4.2.2. Sine Input Condition

Sine input condition at the speed of 60 km/h. The road surface adhesion coefficient is 0.20. The simulation results are shown in Figure 6.
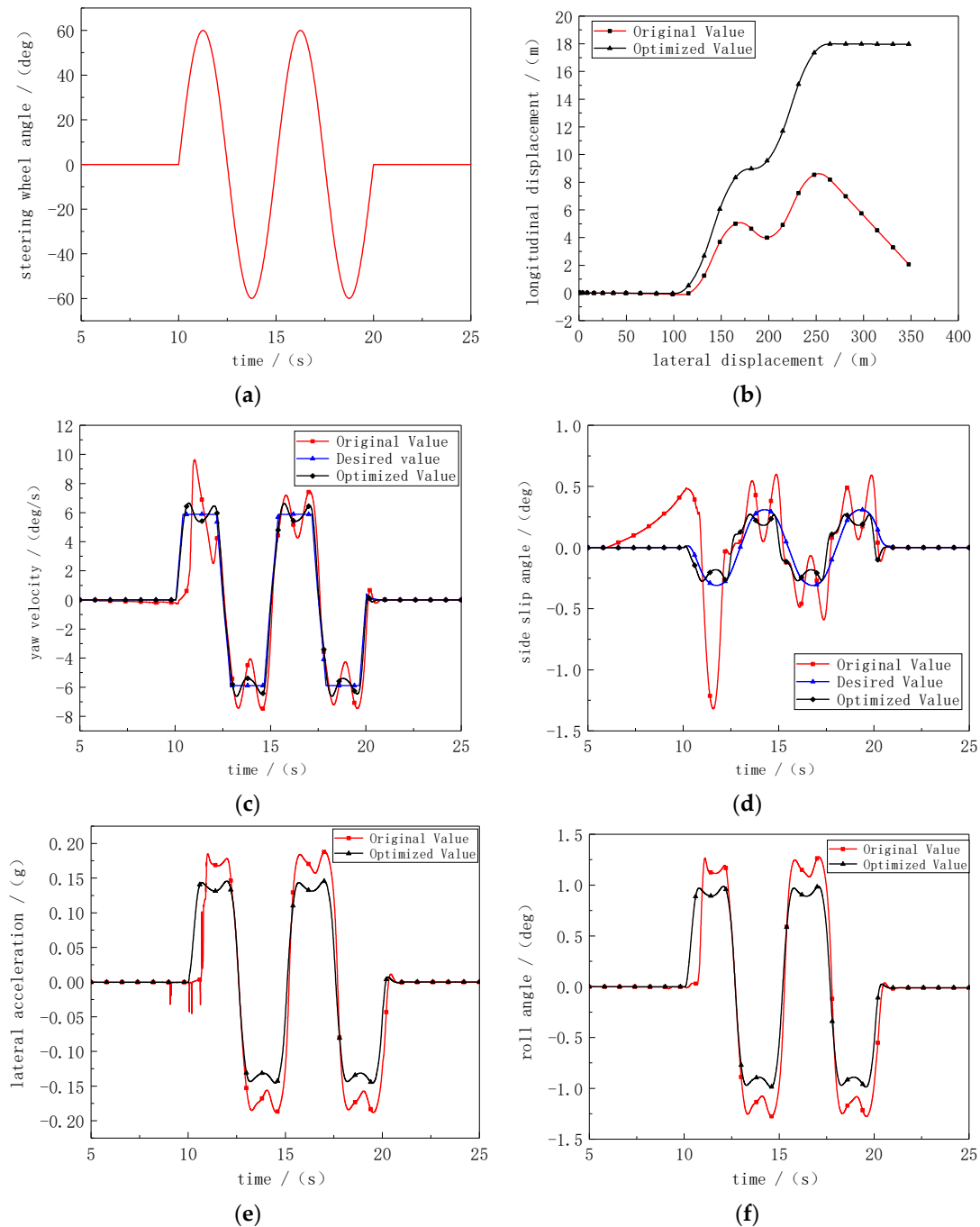
Figure 6. Simulation results of sine input condition. (**a**) Steering wheel angle. (**b**) Vehicle track. (**c**) Yaw velocity. (**d**) Side slip angle. (**e**) Lateral acceleration. (**f**) Roll angle.

Figure 6b shows the driving trajectory curve of the vehicle. Without the control strategy the vehicle has been off tracking; Figure 6c,d show the yaw rate and side slip angle of the vehicle. Both of them have been better corrected with control. It indicates that the vehicle's yaw stability has been improved. Figure 6e,f show the changes of the vehicle's lateral acceleration and roll angle. It can be seen both of them have been significantly reduced.

4.2.3. Fish Hook Test Condition

Fish hook test condition at the speed of 60 km/h. Let the vehicle turn left sharply for 160° at 10 s, and then quickly turn right for 320°. The road surface adhesion coefficient is 0.20. The simulation results are shown in Figure 7.
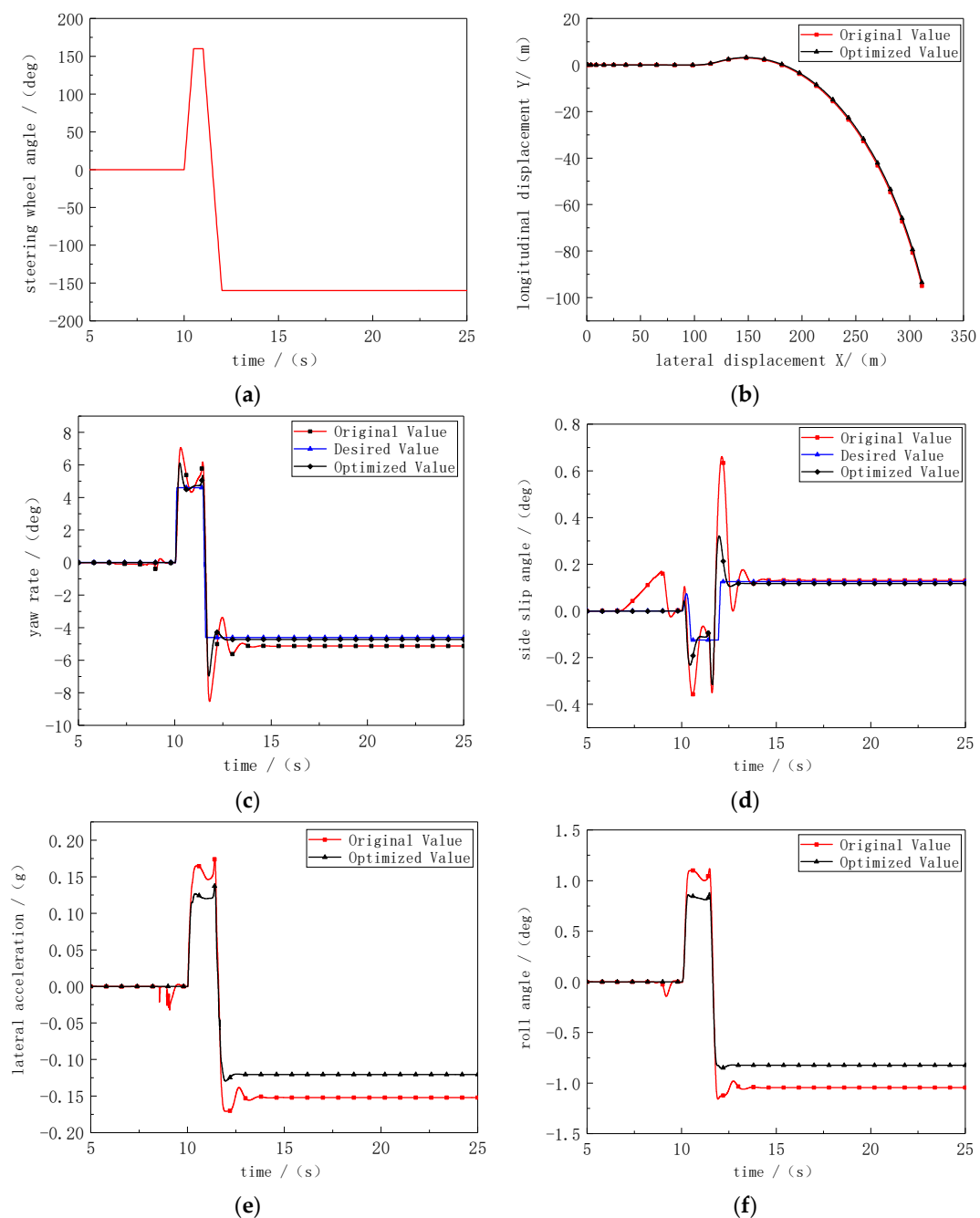
Figure 7. Simulation results of fish hook test condition. (**a**) Steering wheel angle. (**b**) Vehicle track. (**c**) Yaw rate. (**d**) Side slip angle. (**e**) Lateral acceleration. (**f**) Roll angle.

Figure 7c,d show the curves of the vehicle's yaw rate and side slip angle. It can be seen that the vehicle is not seriously stability at this time, and the control strategy of the vehicle's yaw rate is ideal to track the expected value changes while there is a large deviation in the yaw rate and side slip angle without control. Figure 7e,f show the curves of the lateral acceleration and roll angle of the vehicle. After the control strategy is applied, both of them have been better corrected, indicating that the roll yaw control strategy designed in this paper is feasible.

4.3. Simulation Verification of Anti-Rollover Control Algorithm

High-speed sharp turning will cause the vehicle to roll over. Therefore, J-Turn condition and fish hook condition are used as test conditions for simulation verification.

4.3.1. J-Turn Condition

Let the vehicle turn left sharply for 120° at the speed of 80 km/h. It make the vehicle enter the J-turn condition. The road surface adhesion coefficient is 0.85. The simulation results are shown in Figure 8.

It can be seen from Figure 8a,b the LTR value of the vehicle that will reach 0.8 at about 9.5 s and about 1 at 13 s without control. It indicates that the vehicle has already experienced serious roll. At about 17.5 s, the vehicle rolls over. But the LTR value does not fluctuate significantly with control. It keep stable at around 0.8 at 13 s and then remains stable. The vehicle does not roll over. The lateral acceleration reaches 0.78 g at 10 s without control in Figure 8c. Such a large lateral acceleration will inevitably cause the vehicle to generate a greater centrifugal force. At 17.5 s, the curve disappears. It indicates that the vehicle has roll over. The lateral acceleration is significantly reduced and remains stable with control. Figure 8d is the roll angle curve of the vehicle. It can be intuitively judged from the change of the vehicle's roll angle that the body's roll attitude has been significantly suppressed. The controlled roll angle will stabilize at 4.5° after entering the J-turn, while the uncontrolled vehicle roll angle will continue to increase until vehicle roll over. Figure 8e,f are the changes of the vertical load of the four wheels before and after the control. The vertical load of uncontrolled vehicle wheels fluctuates greatly, and the vertical load of the left wheel decreases rapidly after entering a turn. The vertical load of the left rear wheel even drops to 0 which indicates the left rear wheel left the ground. After about 17 s, the vehicle rolls over and all four curves disappear, and the vertical load of the right wheel of the vehicle is significantly reduced with control, especially the peak load of the right front wheel has dropped to about 9000 N. In summary, the anti-rollover control strategy applied to DDEV in this paper is basically effective and feasible under the J-turn operating condition.
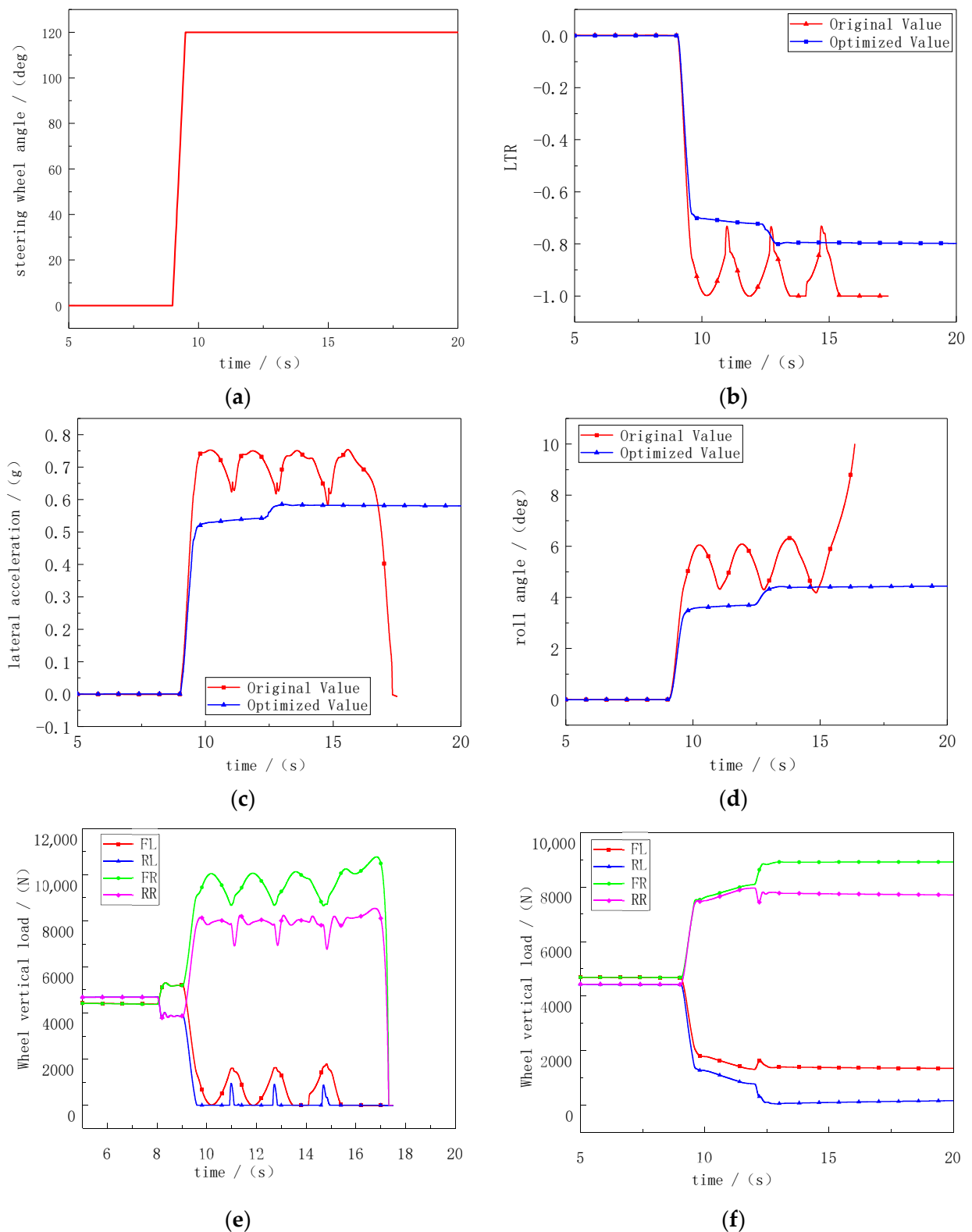
Figure 8. Simulation results of J-turn condition. (**a**) Steering wheel angle. (**b**) LTR. (**c**) Lateral acceleration. (**d**) Roll angle. (**e**) Wheel vertical load before control. (**f**) Wheel vertical load after control.

4.3.2. Fish Hook Test Condition

Fish hook input at the speed of 80 km/h. The road surface adhesion coefficient is 0.85. The simulation results are shown in Figure 9.
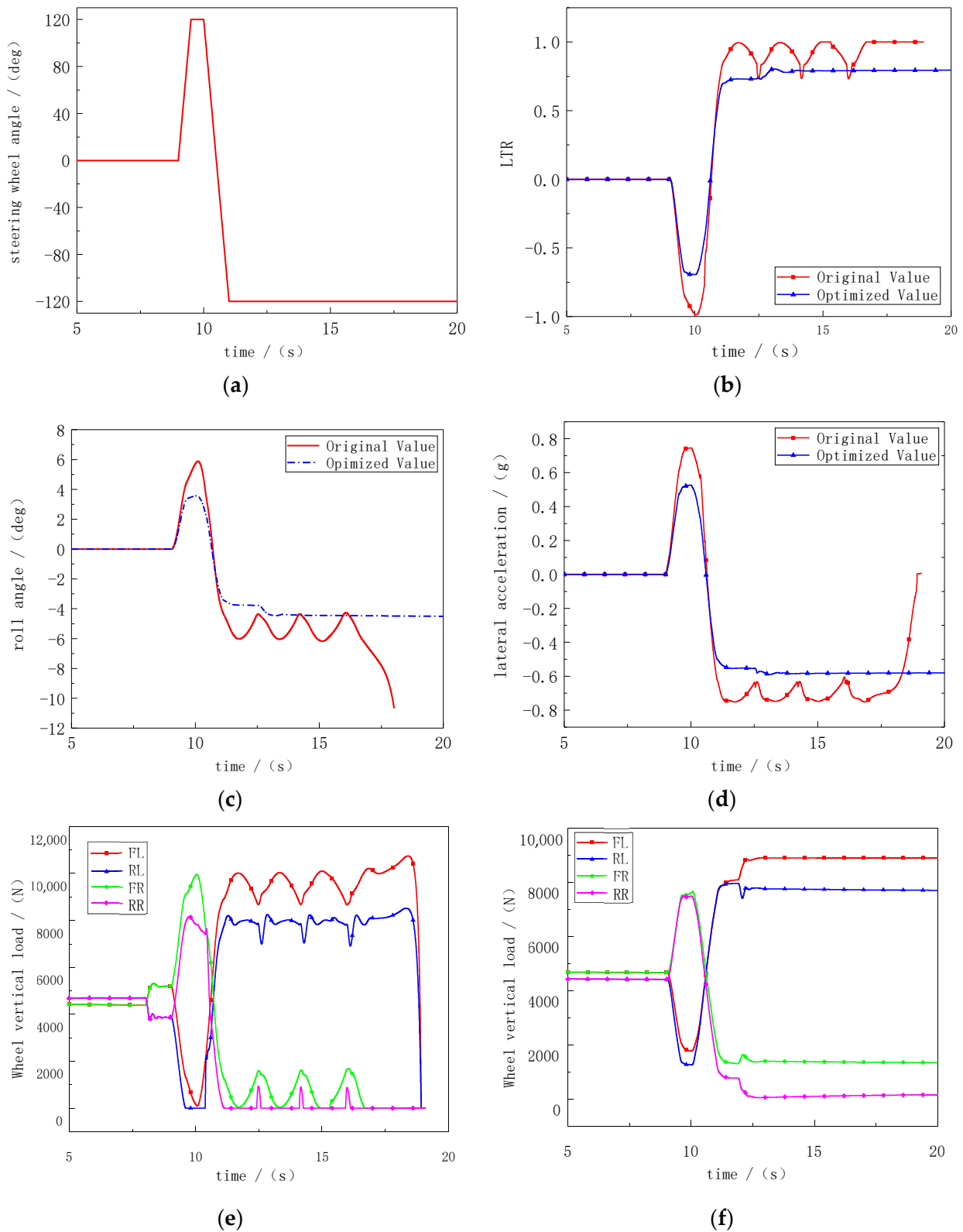
Figure 9. Simulation results of fish hook test condition. (**a**) Steering wheel angle. (**b**) LTR. (**c**) Lateral acceleration. (**d**) Roll angle. (**e**) Wheel vertical load before control. (**f**) Wheel vertical load after control.

Figure 9b shows that the LTR value fluctuates greatly without control. With control the LTR decreases by about 20%, and the curve changes smoothly and stabilizes at 0.8 s. It can be seen from Figure 9c the peak value of lateral acceleration drops from 0.8 g to 0.5 g

with control, and the vehicle no longer rolls over. The lateral acceleration finally stabilizes at 0.55 g. Figure 9d shows the curve of the roll angle of the vehicle. The roll angle continues to increase until the vehicle rolls over without control. The peak value of the roll angle decreases significantly with control. The roll angle at the 20 s still stable at 4.5°. It indicates that the vehicle did not roll over at this time. Figure 9e,f show the changes of the vertical load of the four wheels before and after the control. The vertical load no longer fluctuates greatly with control Moreover, after the vehicle enters a right turn, the peak value of the inner wheel increases, and there is no 0 value. The vertical load of the outer wheel also decreases from 11,000 N at the maximum peak to 9000 N. The vehicle can maintain stable driving without rollover phenomenon.

Therefore the simulation results show that the differential braking anti-rollover control strategy proposed for DDEV in this paper can effectively prevent the vehicle from rolling over under high-speed sharp turns.

5. Conclusions

(1) Active distribution of wheel drive torque will affect both the roll and yaw movements of the vehicle, a decoupling control strategy for roll and yaw is proposed. The yaw stability controller and the roll stability controller are designed based on the LQR control theory and the sliding mode control theory. The control strategy of the compensated yaw and roll moment is evenly distributed in the left and right wheels.

(2) For maneuvering rollover caused by excessive lateral acceleration, an anti-rollover control strategy based on differential braking is designed. The vehicle generates a reverse yaw moment to achieve the control effect of reducing vehicle speed and changing steering characteristics by separately applying a braking torque to the front outer wheel. The lateral load transfer rate is used as the main evaluation index to simulate the typical working conditions. It shows that the differential braking anti-rollover control strategy proposed for DDEV is effective.

Author Contributions: Methodology: S.Y.; formal analysis: S.H. and Y.M.; Preparation of the original draft: X.C.; Writing review and editing: H.Z. All authors have read and agreed to the published version of the manuscript.

Data Availability Statement: Not applicable.

Nomenclature

Symbol	
I_x (kg·m^2)	rotational inertia of the vehicle around the x axis
ϕ (deg)	vehicle roll angle
m_s (kg)	vehicle sprung mass
h_s (m)	distance from the center of the sprung mass to the roll center of the car
b (m)	distance from center of mass to rear axle
a (m)	distance from center of mass to front axle
m (kg)	vehicle mass
v_y (km/h)	vehicle lateral speed
v_x (km/h)	vehicle longitudinal speed
a_y (m/s^2)	vehicle lateral acceleration
ω (rad/s)	angular velocity of the wheel
k_r, k_f (N/rad)	cornering stiffness of the rear and front wheel
L (m)	vehicle wheelbase
r (m)	wheel rolling radius
B (m)	track width

δ (deg)	front wheel angle
K	stability factor
g_y (m/s^2)	gravitational acceleration
F_{yf}, F_{yr} (N)	side force of vehicle front and rear wheels
K^ϕ (N/rad)	equivalent roll stiffness of the car
C^ϕ (N/(km/h))	equivalent roll damping of automobile
ΔM_X (N·m)	additional roll moment.
F_{x1} (N)	ground driving force
T_1 (N·m)	motor torque transmitted from the front wheel to the vehicle body via the suspension
P_{Li} (i = 1, 2, 3, 4) (N)	force exerted by the left body on the front suspensions
P_{Li} (i = 1, 2, 3, 4) (N)	force exerted by the front suspensions on the left body
P_{ij} (j = 1, 2) (N)	force exerted by the car body on the side of the front-inner suspension
P_{ij} (j = 1, 2) (N)	force exerted by the front-inner suspension on the car body
$P_{oi}{}'$ (j = 1, 2) (N)	force exerted by the front-outer suspension on the car body
K_i (i = 1, 2, 3, 4, 5, 6)	the corresponding coefficient of the roll moment
z_i (i = 1, 2, 3, 4) (m)	the corresponding distance
z_{ij} (j = 1, 2) (m)	
l_{out}, l_{in} (m)	
θ_i (i = 1, 2, 3, 4) (rad)	
θ_{ij} (j = 1, 2) (rad)	the corresponding angle
θ_{oi} (i = 1, 2) (rad)	
M_{Xj} (j = 1, 2, 3, 4) (N·m)	roll moment generated by the suspension to the vehicle body
M_{Xi}, M_{Xo} (N·m)	roll moment generated by the front wheel via the suspension
ω_r (dge/s)	vehicle yaw rate
ω_{rd} (dge/s)	ideal yaw rate
ω_{rmax} (dge/s)	the maximum values of yaw rate
β_d (dge)	ideal side slip angle
β_{rmax} (dge)	the maximum values of side slip angle
ξ	weight coefficient between the roll angle and roll angular velocity
e (dge)	the error of roll angle
η	switching gain
μ	road adhesion coefficient
sat (s)	the saturation function
ΔF_{xi} (i = 1, 2, 3, 4) (N)	increment of each driving force
ΔT_i (i = 1, 2, 3, 4)	wheels drive torque
T_{max} (N·m)	maximum driving moment of the motor
F_b (N)	braking force exerted on the front outer wheel
I_w (kg·m^2)	rotating inertia of front outer wheel
T_b (N·m)	vehicle braking torque.
F_{zi} (i = 1, 2, 3, 4) (N)	wheels vertical load
P	braking pressure
S	braking efficiency coefficient.

References

1. Chakraborty, S.; Kumar, N.M.; Jayakumar, A.; Dash, S.K.; Elangovan, D. Selected Aspects of Sustainable Mobility Reveals Implementable Approaches and Conceivable Actions. *Sustainability* **2021**, *13*, 12918. [CrossRef]
2. Boada, B.L.; Boada, M.J.L.; Vargas-Melendez, L. A robust observer based on H ∞ filtering with parameter uncertainties combined with neural networks for estimation of vehicle roll angle. *Mech. Syst. Signal Process.* **2018**, *99*, 611–623. [CrossRef]
3. Zhou, B.; Lü, X.N.; Fan, L. Integrated control of active suspension system and active roll stabilizer. *China Mech. Eng.* **2014**, *14*, 1978–1983.
4. Chen, S.; Xia, C.G.; Pan, D.Y. A study on hybrid rollover control of vehicle with active anti-roll bar. *Automot. Eng.* **2017**, *39*, 667–674.
5. Parsons, K.G.R.; Pask, M.; Burdock, W. The development of ACE for discovery II. In Proceedings of the SAE 2000 World Congress, Detroit, MI, USA, 6–9 March 2000.
6. Karnopp, D. Active and semi-active vibration isolation. *Curr. Adv. Mech. Des. Prod. VI* **1995**, *117*, 409–423.

7.   Xiao, L.J.; Wang, M.; Zhang, B.J. Vehicle roll stability control with active roll-resistant electro-hydraulic suspension. *Front. Mech. Eng.* **2020**, *15*, 43–54. [CrossRef]

8.   Yakub, F.; Abu, A.; Mori, Y. Enhancing the yaw stability and the manoeuvrability of a heavy vehicle in difficult scenarios by an emergency threat avoidance manoeuvre. *Proc. Inst. Mech. Eng. Part D J. Automob. Eng.* **2017**, *231*, 615–637. [CrossRef]

9.   Lua, C.A.; Castillo-Toledo, B.; Cespi, R.; Gennaro, S.D. Nonlinear observer-based active control of ground vehicles with non negligible roll dynamics. *Int. J. Control Autom. Syst.* **2016**, *14*, 743–752. [CrossRef]

10.   Dal Poggetto, V.F.; Serpa, A.L. Vehicle rollover avoidance by application of gain-scheduled LQR controllers using state observers. *Veh. Syst. Dyn.* **2016**, *54*, 191–209. [CrossRef]

11.   Imine, H.; Fridman, L.M.; Madani, T. Steering control for rollover avoidance of heavy vehicles. *IEEE Trans. Veh. Technol.* **2013**, *61*, 3499–3509. [CrossRef]

12.   Chen, B.C.; Peng, H. Differential-braking-based rollover prevention for sport utility vehicles with human-in-the-loop evaluations. *Veh. Syst. Dyn.* **2001**, *36*, 359–389. [CrossRef]

13.   Solmaz, S.; Akar, M.; Shorten, R. Adaptive rollover prevention for automotive vehicles with differential braking. *IFAC Proc. Vol.* **2008**, *41*, 4695–4700. [CrossRef]

14.   Feng, F. Study on Roll Stability of Electric Wheel Drive Vehicle on Uneven Pavement. Master's Thesis, Yanshan University, Qinhuangdao, China, 2017.

15.   Li, G.; Zong, C.F.; Chen, G.Y.; Wei, H.; Lei, H. Integrated control for X-by-wire electric vehicle with 4 independently driven in-wheel motors. *J. Jilin Univ. (Eng. Technol. Ed.)* **2012**, *42*, 796–802.

16.   Wang, Z. The Integrated Control of Active Suspension and Drive Force Distribution Based on 4 In-Wheel Motor Driven Electric Vehicle. Master's Thesis, Southeast University, Nanjing, China, 2016.

17.   Kiyotaka, K.; Toshiyuki, U.; Yoichi, H. Normal force stabilizing control using small EV powered only by Electric double layer capacitor. *World Electr. Veh. J.* **2008**, *1*, 62–67.

18.   Fujimoto, H.; Sato, S. Pitching control method based on quick torque response for electric vehicle. In Proceedings of the 2010 International Power Electronics Conference, Sapporo, Japan, 21–24 June 2010.

19.   Kawashima, K.; Uchida, T.; Hori, Y. Rolling stability control of in-wheel electric vehicle based on two-degree-of-freedom control. In Proceedings of the IEEE International Workshop on Advanced Motion Control, Trento, Italy, 26–28 March 2008.

20.   Kawashima, K.; Uchida, T.; Hori, Y. Rolling stability control based on electronic stability program for in-wheel-motor electric vehicle. *World Electr. Veh. J.* **2009**, *3*, 34–41. [CrossRef]

21.   Katsuyama, E. Decoupled 3D moment control using in-wheel motors. *Veh. Syst. Dyn.* **2013**, *51*, 18–31. [CrossRef]

22.   Murata, S. Innovation by in-wheel-motor drive unit. *Veh. Syst. Dyn.* **2012**, *50*, 807–830. [CrossRef]

23.   Yu, Z.S. *Automobile Theory*, 5th ed.; China Machine Press: Beijing, China, 2009.

24.   Liu, B.; Tang, W.S. *Modern Control Theory*; China Machine Press: Beijing, China, 2006.

25.   Zhang, X.Z.; Zheng, L. Vehicle stability control of distributed-driven electric vehicles based on optimal torque allocation. *China Mech. Eng.* **2018**, *29*, 1780–1787.

26.   Ren, Z.Y.; Zhao, W.Q.; Zong, C.F. Research on vehicle yaw stability control based on improved LQR method. *Sci. Technol. Eng.* **2017**, *17*, 97–102.

27.   Yan, S. Research on Roll Stability Control of Distributed Drive Electric Vehicle. Master's Thesis, Shanghai University of Engineering Science, Shanghai, China, 2020.